Original Paper

Use Dependent Attenuation of Rat HCN1-Mediated I_h in Intact HEK293 Cells

Lennart Barthel   Olivia Reetz   Ulf Strauss

Institute of Cell Biology and Neurobiology, Charité-Universitätsmedizin Berlin, Berlin, Germany

Abstract

Background/Aims: Cationic currents (I_h) through the fast activating and relatively cAMP insensitive subtype of hyperpolarization-activated cyclic nucleotide-gated (HCN) channels, HCN1, are limited by cytosolic factors in mammalian cells. This cytosolic HCN1 break is boosted by changes in membrane voltage that are not characterized on a biophysical level, yet. ***Methods:*** We overexpressed rat (r)HCN1 in human embryonic kidney cells (HEK293) and recorded pharmacologically isolated I_h in cell-attached or whole-cell mode of the patch-clamp technique. ***Results:*** Recurring activation of rHCN1 reduced and slowed I_h in intact HEK293 cells (cell-attached mode). On the contrary, sustained disruption of the intracellular content (whole-cell mode) ceased activity dependence and partially enables voltage dependent hysteresis. The activity induced I_h attenuation in intact cells was independent of the main external cation, depended on the number of previous forced activations and was - at least in part - due to a shift in the voltage dependence of activation towards hyperpolarization as estimated by an adapted tail current analysis. Intracellular elevation of cAMP could not reverse the changes in I_h. ***Conclusion:*** Reduction of rHCN1 mediated I_h is use dependent and may involve the coupling of voltage sensor and pore.

© 2016 The Author(s)
Published by S. Karger AG, Basel

Introduction

Tetrameric HCN channels belong to the family of voltage gated ion channels and – contrary to most other channels – are activated by hyperpolarization. The fourth of the six trans-membrane segments (S4) acts as voltage sensor and coupling of this voltage sensor with the pore (S6) is mediated by an interaction of S4-S5 linker and C-linker [1]. Besides its canonical pacemaking action in cardiac myocytes [2] HCN-mediated, mixed inward rectifying cation current I_h in neurons contributes to setting excitability levels, resonance

Ulf Strauss   Institute of Cell Biology and Neurobiology, Center for Anatomy, Charité-
Universitätsmedizin Berlin, Charitéplatz 1, 10117 Berlin, (Germany)
Tel. +4930 450528434, Fax +4930 450528902, E-Mail ulf.strauss@charite.de

KARGER

Cellular Physiology and Biochemistry

Cell Physiol Biochem 2016;38:2079-2093

DOI: 10.1159/000445566
Published online: May 17, 2016

© 2016 The Author(s). Published by S. Karger AG, Basel
www.karger.com/cpb

2080

Barthel/Reetz/Strauss: HCN1 Use Dependence

and synchrony [3]. Due to its opening at voltages close to the resting membrane potential it depolarizes the membrane on the one hand but reduces the membrane resistance on the other influencing amplitude, summation and time course of postsynaptic potentials [4]. Particularly the latter actions depend not only on current amplitude but also on activation kinetics of the channels involved. The fastest activating of the four known mammalian HCN subunits (HCN1-4), HCN1, is widely expressed in the hippocampus, cerebellum and neocortex [5] and is of vast importance for regulating dendritic integration [6, 7].

In general, the opening of HCN channels is supported by binding of cyclic nucleotides such as cAMP or cGMP to a C-terminal intracellular cyclic nucleotide binding domain [3], in particular in channels containing HCN2 and HCN4 subunits. However, the effect of cAMP on HCN1 is much weaker: cAMP depolarizes the voltage dependence of activation for HCN2 and 4 about 10 - 20 mV but only about 2 - 5 mV for HCN1 [2, 8, 9]. Nevertheless, an opening transition of HCN channels might be allosterically coupled to conformational changes in the cyclic nucleotide binding domain (CNBD) and therewith enhance the cAMP sensitivity of the channels open state as predicted by a six state cyclic allosteric model [10]. Consistent with that model, activating mouse HCN1 channels facilitates I_h by depolarizing its voltage dependence as revealed in intact frog oocytes (by recordings in 2 electrode voltage clamp) [11]. This depolarizing shift might be pronounced under certain conditions (up to +60 mV) preventing arrhythmic firing in model cells of sino-atrial node [11]. We previously found that in intact mammalian cells (HEK293) (by recordings in cell-attached mode) strong hyperpolarizations led to a reduction of maximum rat (r)HCN1 mediated I_h [12]. This I_h attenuation depended on an intact cytosol (cell-attached patch clamp) and may underlie the enhancement of maximum I_h and the depolarizing shift after disrupting the intracellular content, i. e. establishment of whole-cell mode. Increasing intracellular cAMP or phosphorylation in whole-cell mode did not restore this cytosol-dependent I_h modulation. The importance of I_h modulations in physiological and pathophysiological context [13-16] prompted us to shed further light on this controversy. To closer investigate biophysical determinants of the I_h reduction we here expressed rHCN1 in mammalian HEK293 cells.

Our results indicate that I_h attenuation depends on recurring activation but does not occur after disrupting the cell membrane in whole-cell mode. Moreover, the inactivation depends stronger on the number of activations than on the activating voltage. A shift in voltage dependency seems to promote this effect.

Materials and Methods

Cell culture

HEK293 cells (DSMZ, Braunschweig, Germany) were used as a transient expression system, because they contain a small number of endogenous voltage gated ion channels [17] that can be easily blocked. Thus, currents through transfected channels can be recorded independently. Cells were cultured at 37°C (95% O_2, 5% CO_2) in Dulbecco´s modified eagle medium (DMEM, P04-03550, Pan-Biotech GmbH, Aidenbach, Germany) supplemented with 1% L-glutamine, 4,5 g/L D-glucose, 10% fetal calf serum, 1% penicillin/streptomycin (Pan-Biotech GmbH, Aidenbach, Germany) and 3.7 g/L $NaHCO_2$. Cells were detached mechanically with pre-warmed DMEM and passaged every second to fourth day. One day after plating on poly-L-lysine coated coverslips cells were transfected with the previously described pIRES2_dsRed-rHCN1 [12] by incubation with 2 M $Ca_3(PO_4)_2$. Optimal transfection rates were obtained by incubation for 7 to 14 minutes. Sequences were confirmed by restriction analyses, sequencing, and subsequent database alignments.

Patch-clamp-recordings

Coverslips with HEK293 cells were transferred into a recording chamber 2 - 4 days after transfection. The cells were constantly perfused with extracellular solution (in mM): 120 NaCl, 10 KCl, 0.5 $MgCl_2$, 10 HEPES, 10 glucose (Carl Roth GmbH and Co. Kg, Karlsruhe, Germany), 1.8 $CaCl_2$ (Merck, Darmstadt, Germany), 10 TEA and 2.5 4-aminopyridine (Sigma-Aldrich, Munich, Germany). pH was set to 7.4 with NaOH. Discretely located rHCN1-overexpressing HEK239 cells were identified by red fluorescence on an inverted

KARGER

2081

Barthel/Reetz/Strauss: HCN1 Use Dependence

microscope (Axiovert S100; Zeiss, Oberkochen, Germany) equipped with an EC Plan-Neofluar 20x/0,50 Pol M27 objective. Pulled glass pipettes had a resistance of 2 - 4.7 MΩ (P-97 micropipette puller; Sutter Instruments, Novato, CA, USA). Pipette solution for experiments in whole-cell mode contained (in mM): 120 K-methylsulphate (KMeSO$_4$), 20 KCl, 14 Na-phosphocreatine, 0.5 EGTA, 4 NaCl, 10 HEPES, 4 Mg^{2+} - ATP, 0.3 Tris-GTP, 0.1 cAMP. Pipette solution for cell-attached recordings matched the one of our previous studies [12, 18] and the studies of others, e. g. [19] to enable comparison as well as to increase I_h and contained (in mM): 120 K-gluconate, 11 EGTA, 10 Na-phosphocreatinine, 0.3 Tris-GTP, 2 Mg^{2+} ATP, (Sigma Aldrich), 10 KCl, 1 MgCl$_2$, 1 CaCl$_2$, 10 HEPES. Solutions were set to pH 7.2 with KOH (Carl Roth) and kept on ice. High pipette content of K$^+$ increases the permeability of HCN channels [20-22], therewith enabling robust cell attached measurements and improving the signal to noise ratio [23]. Conductance of HCN channels is very sensitive to changes in the extracellular potassium concentration [24]. A high extracellular K$^+$ concentration therefore might prevent putative HCN decline due to depletion or some decrease in extracellular K$^+$. For experiments with high extracellular Na$^+$, the pipettes were filled with extracellular solution as used for perfusion in all other experiments and given above. Experiments were conducted at room temperature (21 - 24C°). Cell-attached recordings were only performed when the total resistance (seal resistance and patch resistance) was > 2 GΩ. After establishing whole-cell mode, cells were given ~2 minutes for recovery and substitution of intracellular fluid with pipette solution.

Data and Statistical Analyses

Experiments were recorded with an EPC-10 amplifier (HEKA, Lambrecht, Germany), controlled by Patch-Master software v2.23 (HEKA). Data were filtered by a Bessel-filter with 3 kHz and sampled with 10 kHz. Offline analysis was conducted with FitMaster v2.67 (HEKA) and Origin8.5 (Origin Labs, Northampton, MA, USA). Liquid junction potentials (9.3 mV) were not corrected for. HEK293 cells were used as transfection system because confounding currents activated by hyperpolarization were low in our hands (see above and [12], Fig. 2B, therein). In addition putative (confounding) ionic conductances were blocked. Although all this does not entirely exclude any non-HCN conductance (unresolved conductance pathways in the patch) contributing to instantaneous currents, "leak" currents in the cell-attached configuration were not subtracted. I_h and I_{inst} amplitudes were determined between dotted lines shown in Fig. 1A. For whole-cell measurements linear leak current was subtracted. In case of n < 8 or non-normal data distribution, non-parametric tests for paired samples (Wilcoxon-signed rank test) or non-paired samples (Mann Whitney U test) were used. When n ≥ 8 and data were normally distributed, paired t tests were performed. Tail current amplitudes were normalized separately for every single patch, resulting data were fitted with the Boltzmann equation: $I(V) = ([A1 - A2]/1+ e ([V-V1/2]/k)+A2)$. Results were considered as significant if p < 0.05. Error bars of means represent SEMs.

Results

I_h of intact HEK293 cells decreased after recurring activation irrespective of singular long channel pre-activation

Whereas in *Xenopus* oocytes HCN1 activation induced an up to +60 mV depolarizing shift in voltage dependent activation [11] we found a pre-pulse dependent amplitude reduction of HCN1 mediated I_h in intact mammalian HEK293 cells [12].

We set out to find determinants of and to biophysically characterize this I_h reduction. Recurring I_h activations by hyperpolarizing the membrane every 10 seconds from a holding potential of 0 mV to –100 mV for 1 second in cell-attached mode rapidly reduced the I_h amplitude. In detail, 10 such hyperpolarizations reduced the I_h amplitude by 30.3 ± 2.7% (n = 23, p < 0.001, Wilcoxon-signed rank test, Fig. 1A). The reduction remained unchanged after 20 activations (by 39.4 ± 3.4% *vs.* 35.8 ± 3.2% n = 9, p = 0.1, paired t test), after 30 activations (by 42.4 ± 1.3% *vs.* 35.5 ± 6.7%, n = 4, p = 0.4, Wilcoxon-signed rank test) or after 50 activations (by 45.2 ± 2.5% *vs.* 37.2 ± 0.99%, n = 2) when compared to the value after 10 activations of the respective patch. Repetitive hyperpolarizations also attenuated the instantaneous current component (I_{inst}) after 10 activations by 28.4 ± 3.4%, n = 23, p < 0.001, Wilcoxon signed rank test, Fig. 1A) with no further changes after 20 (by 34.8 ± 5.9% *vs.* 35.3

KARGER
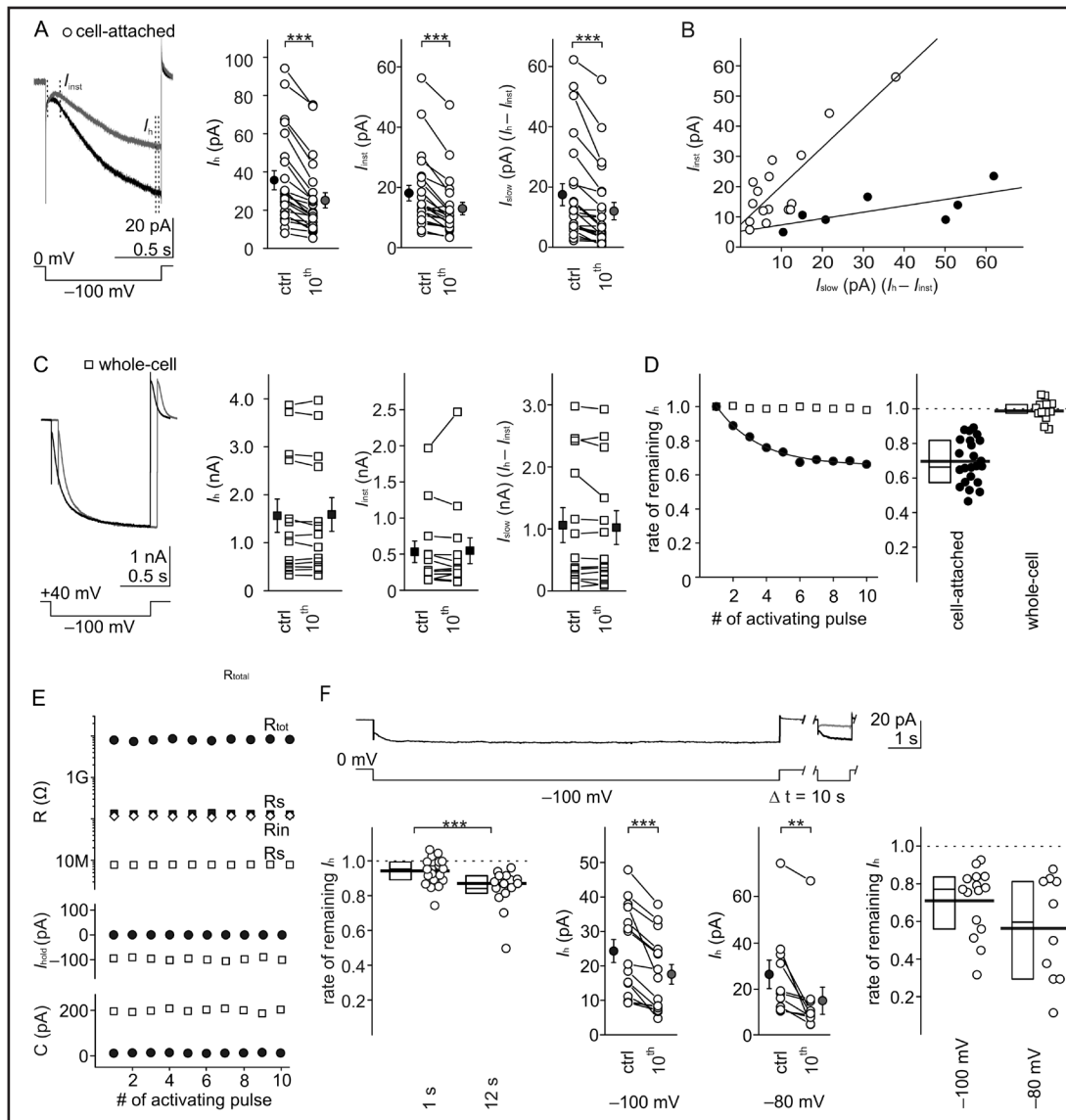
Fig. 1. Repetitive rHCN1 channel activation reduces I_h amplitude in intact HEK293 cells. (A) Left: Overlay of example traces of rHCN1-mediated I_h, elicited by hyperpolarizing voltage steps in cell-attached mode. We repetitively stepped for 1 second to –100 mV in intervals of 10 seconds (bottom) and show the first (black) and tenth (grey) current trace including measuring intervals for I_h and I_{inst}. Right: Population data of amplitudes of I_h (*left*), I_{inst} (*middle*) and slowly activating components ($I_{slow} = I_h - I_{inst}$, *right*) of first (*ctrl*) and 10th recordings. (B) Plotting I_{inst} against I_{slow} amplitudes revealed two strong linear correlations ($y = a + b * x$) indicative for distinct distribution of time dependent and permanently open channels in different patches. Intercepts indicate the amount of instantaneous current, expected in HEK293 cells without rHCN1 expression. White circles: $I_{inst}/I_{slow} > 1$; black circles: $I_{inst}/I_{slow} < 1$. (C) I_h reduction depends on intact cytosol. Left: Overlay of 1st and 10th traces from rHCN1 overexpressing HEK293 cells, recorded in whole-cell configuration starting 3 minutes after rupturing the membrane. For better differentiability 10th trace is shifted slightly rightward. We repetitively activated I_h by a 1 second voltage pulse to –100mV from a holding potential of +40 mV (bottom). Right: Population data reveal no alterations of I_h (left), I_{inst} (middle) or I_{slow} (right) after 10 consecutive activations. (D) Left: Course of I_h reduction in two example HEK293 cells, one recorded in cell-attached mode (black circles) and one in whole-cell mode (white squares). We normalized I_h of individual traces to the respective control I_h (first trace). The solid black curve represents a single exponential fit to the course of I_h decay. Right: Amount of I_h reduction (rate of remaining I_h) given as I_h at the 10th voltage pulse normalized to its initial value (i.e. at the first voltage pulse). Note that in cell-attached mode (black circles)

KARGER

Cellular Physiology and Biochemistry

Cell Physiol Biochem 2016;38:2079-2093

DOI: 10.1159/000445566
Published online: May 17, 2016

© 2016 The Author(s). Published by S. Karger AG, Basel
www.karger.com/cpb

2083

Barthel/Reetz/Strauss: HCN1 Use Dependence

the rate of remaining I_h dropped substantially, but it resided close to 1 in whole-cell mode (white squares). (E) Time course of experimental patch parameters input (R_{in}) and series resistance (R_s) as well as total resistance (R_{tot}), holding current (I_{hold}) and cell and patch capacitance (C) exemplified for the whole cell and cell attached recording shown in 1D, respectively. (F) I_h reduction in cell-attached recordings depends more on repetitive stimulation than on voltage. Upper row: After a prolonged (12 seconds) activating voltage of –100 mV (*top*) we applied repetitive 1 second steps to –100 mV every 10 seconds as in A. Lower row: Long pre-activation to –100 mV changed the reduction of the subsequent pulse compared with a short pre-activation (bottom, left panel). Population data reveal that pre-activation did not influence the rate of remaining I_h compared to A as estimated by 1 second activations following long pre-activation (bottom panels). Throughout this and the following figures error bars represent SEM and *p < 0.05, **p < 0.01, ***p < 0.001. Individual data are summarized as 25 - 75% box plots, thick lines trough boxes and individual data represent means and thin lines within the boxes represent medians.

± 4.12% n = 9, p = 0.9, paired t test), after 30 activations (by 43.7 ± 10.7% *vs.* 37.2 ± 8.7%, n = 4, p = 0.6, Wilcoxon-signed rank test) or after 50 activations (by 39.0 ± 17.6% *vs.* 23.2 ± 7.4%, n = 2) when compared to the value after 10 activations of the respective patch. This indicates that a steady state has been reached in most cases after 10 to 20 HCN channel activations.

I_h reductions in our cell-attached recordings are unlikely due to alterations in the experimental setting because none of the commonly estimated parameters (exemplified in Fig. 1E) as capacitance (C_{ini} = 21.7 ± 2.6 pF vs. C10 = 19.8 ± 3.01 pF, n = 12, p = 0.3, Wilcoxon signed rank test), total resistance (R_{totini} = 7.7 ± 1.3 GΩ vs. 8.1 ± 1.3 GΩ, n = 12, p = 0.5, paired t test), series resistance (R_{sini} = 16.1 ± 2.5 MΩ vs. RS10 = 18.7 ± 3.0 MΩ, n = 12, p = 0.62, Wilcoxon signed rank test) changed throughout the measurements. As a surrogate parameter the holding current remained stable in all recordings throughout the experiments (I_{hold10} = –1.6 ± 0.5 pA vs. $I_{holdini}$ = –1.4 ± 0.5 pA, n = 23, p = 0.66, Wilcoxon signed rank test; I_{hold20} = –1.4 ± 0.6 pA vs. $I_{holdini}$ = –1.0 ± 0.7 pA, n = 9, p = 0.23, Wilcoxon signed rank test; I_{hold30} = –3.0 ± 0.9 pA vs. $I_{holdini}$ = –2.2 ± 1.3 pA, n = 4, p = 1, Wilcoxon signed rank test; I_{hold50} = –3.4 ± 0.14 pA vs. $I_{holdini}$ = –1.3 ± 1.5 pA, n = 2).

The instantaneous component of the current (I_{inst}) may depend on the expression system and its nature is not entirely clear. HCN cannels may conduct a portion of I_{inst} in addition to the well-characterized slowly activating component of I_h since HCN channels produce a background current after heterogeneous expression [25, 26]. I_{inst} has been previously linked to HCN channels by amplitude correlation with the slowly activating I_h component, similar reversal potentials, similar dependence on intracellular Cl⁻, cAMP and on the availability of accessory subunits (for instance MiRP1). In particular, permanently open states have been explicitly shown for HCN2 channels in different expression systems [27, 28] and may be inferred for HCN1 from observations in oocytes [21, 29-31]. In line, the correlation between the certainly HCN1 mediated I_{slow} and the putatively HCN1 co-mediated I_{inst} in our experiments may indicate that expression of HCN1 channels not only generates time dependent but also permanently open channels. Given that attenuation of the slowly activating current component (I_{slow}), i.e. the difference of I_h and I_{inst}, was slightly more pronounced (34.0 ± 5.1%, n = 23, p < 0.001, Wilcoxon signed rank test, Fig. 1A), I_{inst} appeared to be less affected by amplitude reduction. This is underlined by the tendency of rise in relative I_{inst} portion during repetitive hyperpolarizations from I_{inst}/I_{slow} = 1.8 ± 0.3 to I_{inst}/I_{slow} = 2.8 ± 0.75 (n = 23, p = 0.23, Wilcoxon-signed rank test). Correlating I_{inst} and I_{slow} readily divided these two groups (small I_{inst}: I_{inst}/I_{slow} < 1, n = 7, r = 0.65, slope = 0.19, intercept = 6.4 pA; large I_{inst}: I_{inst}/I_{slow} > 1, n = 16, r = 0.86, slope = 1.3, intercept = 6.6 pA) when linearly fit (Fig. 1B). Although this strong linear correlation implies that expression of rHCN1 generates time dependent and permanently open channels in HEK293 cells and the total resistance amounted to 6.4 ± 1.0 GΩ, it does not entirely exclude different levels of unresolved leak currents. Nevertheless, comparing the relative I_{inst} portion before and after repetitive hyperpolarizations further suggests an increase after 10 activations when I_{inst} was large (I_{inst}/I_{slow} = 2.4 ± 0.3 to I_{inst}/I_{slow} = 3.8 ± 1.0, n = 16, p = 0.25, Wilcoxon-signed rank test) but not when I_{inst} was small (I_{inst}/I_{slow} = 0.43 ± 0.07 *vs.* I_{inst}/I_{slow} = 0.48 ± 0.14, n = 7,

KARGER

Cellular Physiology and Biochemistry

Cell Physiol Biochem 2016;38:2079-2093

DOI: 10.1159/000445566
Published online: May 17, 2016

© 2016 The Author(s). Published by S. Karger AG, Basel
www.karger.com/cpb

2084

Barthel/Reetz/Strauss: HCN1 Use Dependence

p = 1, Wilcoxon-signed rank test). This either indicates that the state of permanently open channels (putatively, but not certain rHCN1, see above) or unresolved conductances is less use dependent.

After a break of 10 minutes current amplitudes did not recover, neither for I_h (I_{hini} = 33 ± 7.5 pA $vs.$ I_{h10min} = 20.6 ± 4.6 pA, remaining I_h = 66.3 ± 15.3% $vs.$ 70.6 ± 7.4% after the initial 10 activations, n = 3), nor for I_{inst} ($I_{instinitial}$: 14.5 ± 1.3 pA, to $I_{inst10min}$ = 8.6 ± 2.1 pA, remaining I_{inst}: 47.6 ± 6.7% $vs.$ 61.1 ± 7.8% after the initial 10 activations, n = 3) nor for I_{slow} ($I_{slowinitial}$: 18.5 ± 6.4 pA to $I_{slow10min}$ = 12.0 ± 3.0 pA, remaining I_{slow}: 68.3 ± 7.6% $vs.$ 81.4 ± 11.6 % after the initial 10 activations, n = 3). The holding current was stable ($I_{holdini}$ = −5.4 ± 0.22 pA $vs.$ I_{hold10} = −5.7 ± 0.23 pA, n = 3).

For patches with a distinct I_h reduction the time course of amplitude decrement was relatively fast, as estimated by a fit to a single exponential function (τ_{reduct} = 7.12 ± 2.3 hyperpolarizations, n = 14). In line with our previous report [12], disrupting the cytosolic content by rupturing the membrane prevented the reduction of I_h (remaining I_h: 0.85 ± 1.6%, n = 13, p = 0.5, Wilcoxon-signed rank test), I_{inst} (remaining I_{inst}: −0.6 ± 6.7%, n =13, p = 0.6, Wilcoxon-signed rank test) and I_{slow} (remaining I_{slow}: −1.2 ± 7.7%, n = 13, p = 0.6, Wilcoxon-signed rank test, Fig. 1C) when we waited for 3 minutes after establishing the whole-cell mode to prevent further "run-up" and held the membrane at +40 mV to exclude channel activation. Whereas the rate of remaining I_h after 10 activations by hyperpolarizing voltage pulses was 0.7 ± 0.03 (n = 23) in cell-attached mode, it was 0.99 ± 0.02 in whole-cell mode (n = 13, p < 0.001 when comparing cell attached and whole-cell values by t-test, Fig. 1D). Recording conditions were stable throughout all whole-cell experiments, as capacitance (C_{ini} = 162.9 ± 67.9 pF $vs.$ C_{10} = 180.1 ± 71.7 pF, n = 13, p = 0.3, Wilcoxon signed rank test), input resistance (R_{inini}: 509.4 MΩ ± 116.1 MΩ $vs.$ R_{in10} = 413.5 MΩ ± 91.9 MΩ, n = 13, p = 0.1, paired t test), series resistance (R_{sini} = 9.7 ± 1.04 MΩ $vs.$ R_{s10} = 9.9 ± 1.02 MΩ, n = 13, p = 0.07, Wilcoxon signed rank test) and holding current ($I_{holdini}$ = −8.5 ± 25.5 pA after −7.9 ± 26.3 pA, n = 13; p = 0.09, paired t test) remained stable during the recordings.

Next, we investigated whether the I_h reduction depends on pre-activating voltage. For that we used an activating pulse longer than the total activation time necessary for reducing I_h amplitude to 1/3 (τ_{reduct}), i. e.12 seconds. Subsequently to such long activation we again stepped 10 times to −100 mV (Fig. 1F). Compared to a prior activation of 1 second, the 12-second activation by −100 mV led to a slight but significant reduction of the I_h amplitude elicited by the subsequent pulse (rate of remaining I_h 12 seconds pre-activation: 0.84 ± 0.03, n = 15 $vs.$ 1 second pre-activation: 0.94 ± 0.01, n = 23, p < 0.001, Mann Whitney U test, Fig. 1F). However, repetitive stimulation still reduced the I_h amplitude for pre-activations at −100 mV (by 29.1 ± 4.6%, n = 15, p < 0.001, paired t test) and at −80 mV (by 43.8 ± 8.8 %, n = 10, p < 0.01, Wilcoxon-signed rank test, Fig. 1F). This was also reflected by similar rates of remaining I_h (for −100 mV pre-activation: 0.70 ± 0.05, n = 15, for −80 mV pre-activation: 0.56 ± 0.08, n = 10, Fig. 1F) when compared to rates of remaining I_h without pre-activation (Fig. 1D, p = 0.37, Kruskal-Wallis). In line, the course of I_h amplitude reduction was similar with and without pre-activation and independent of pre-activation voltage (τ_{reduct} after −100mV: 9.9 ± 1.8 hyperpolarizations, n = 15; τ_{reduct} following −80mV pre-activation: 7.8 ± 2.1 hyperpolarizations, n = 10, p = 0.09, Kruskal-Wallis).

The holding current was stable throughout for experiments following −100mV pre-acivation ($I_{holdini}$ = 0.49 ± 0.1 pA $vs.$ I_{hold11} = 0.36 ± 0.09 pA, n = 15, p = 0.17, Wilcoxon-signed rank test) and following −80mV pre-activation ($I_{holdini}$ = 0.5 ± 0.08 pA $vs.$ I_{hold11} = 0.33 ± 0.06 pA, p = 0.14, paired t test).

The data suggest that repetitive stimulation, i.e. sequent channel openings and closures, is a prerequisite for reducing I_h amplitude.

I_h reduction depends more on number of previous activations than on its respective voltage and is accompanied by a hyperpolarized voltage dependence

Given that HCN channel opening is strongly voltage dependent [3], the voltage of each activating step might influence I_h amplitude reduction, even if a prolonged pre-activation
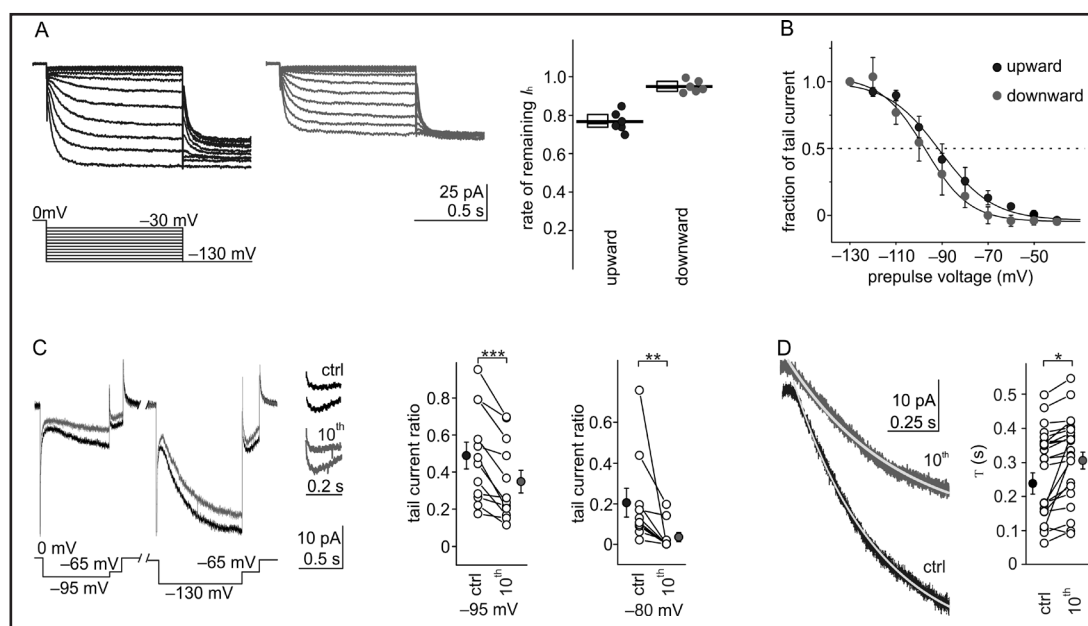
Fig. 2. Reduction of maximum I_h is accompanied by a hyperpolarizing shift in voltage dependence of activation. (A) Left: Consecutive trace families of cell-attached recordings of rHCN1-mediated I_h. We clamped the pipette voltage from –130 mV in 10 mV steps upward to –30 mV (*black traces*) and subsequently downward from –30 mV to –130 mV (grey traces). Each pulse was followed by a 0.5 second long hyperpolarization to –130 mV. Pulse protocol depicted below. Right: Population data on rate of remaining I_h. Note that I_h was normalized to the maximum I_h of the respective family, i.e. in the second family (grey circles) nearly no further I_h reduction occurred. (B) Conventionally estimated voltage dependence of I_h. For I_h families shown in (A) we determined the voltage of half maximal $V_{1/2}$ by normalizing tail currents to its maximal value for each patch, plotted them against pre-pulse voltage and fitted to the Boltzmann equation. For illustration, respective means (black circles for upward, i. e. during I_h reduction, grey circles for downward, i.e. after I_h reduction) are depicted and fitted (n = 6, respectively). (C) Shift of voltage dependent activation accompanies I_h reduction. We roughly determined voltage dependence of I_h activation by a truncated approach, normalizing I_h tail currents at –65 mV after moderately activating pre-pulses of –80mV or –95 mV to those after assumingly fully activating pre-pulses of –100 mV or –130 mV, respectively. Left: example for initial (*ctrl*, black) and 10th (grey) trace and enlarged assigned tail currents illustrating the approach. Right: Population data of tail current ratios for pre-pulses –95 mV (left) and of –80 mV (right) indicate a hyperpolarizing shift in the voltage dependence of I_h activation. (D) I_h activation time course at –100 mV slowed during repetitive activation (left) as revealed by population data on activation time constants of I_h (τ) (right). Grey lines overlaying the example traces (left) indicate fits to single exponential functions.

had a minor effect. Moreover, our first hints for a use dependent I_h amplitude reduction came from a common protocol for eliciting families of I_h, descending membrane voltage from –30 mV to –130 mV for 2 seconds [12]. We here adapted and reversed this protocol, combining a 1 second pre-activation (for better comparability to the repetitive activation at –100 mV) at voltages ascending from –130 mV to –30 mV with 0.5 second (test) steps to –130 mV (Fig. 2A). After one run of this protocol I_h amplitudes were reduced by 23.3 ± 2.1% (n = 6, p < 0.05, Wilcoxon signed rank test), comparable to the reduction after repeated steps to –100 mV (p = 0.13, Mann Whitney U test). In line, the course of I_h amplitude reduction matched the one achieved by stepping repeatedly to –100 mV (τ_{reduct} = 6.2 ± 1.6 hyperpolarizations, p = 0.27, Mann Whitney U test). I_h amplitude reduction was nearly complete as an adjacent second voltage protocol (descending as in [12]) hardly reduced I_h further (by 5.1 ± 1.2 %, n = 6, p < 0.05, Wilcoxon signed rank test). Contrary to our previous conclusion based on a

KARGER

Cellular Physiology and Biochemistry

Cell Physiol Biochem 2016;38:2079-2093

DOI: 10.1159/000445566
Published online: May 17, 2016

© 2016 The Author(s). Published by S. Karger AG, Basel
www.karger.com/cpb

2086

Barthel/Reetz/Strauss: HCN1 Use Dependence

limited number of experiments [12], our current data suggest that pre-pulse voltage does not influence I_h reduction as long as the voltage activates the current.

The holding current did neither change during the first trace family ($I_{holdini}$ = 1.3 ± 0.2 pA *vs.* I_{hold11} = 1.2 ± 0.2, n = 6, p = 0.68, Wilcoxon signed rank test) nor during the subsequent family ($I_{holdini}$ = 1.2 ± 0.3 pA *vs.* I_{hold11} = 1.0 ± 0.2 pA, n = 6, p = 0.4, Wilcoxon signed rank test). On the other hand, I_h activation might influence voltage dependence of HCN channel gating as indirectly supported by our previous experiments: conventional tail current analysis revealed a voltage of half maximal I_h activation ($V_{1/2}$) of –92.4 mV during the process of I_h amplitude reduction [12] and –96 mV after this reduction was settled [18]. However, experimental conditions in these sets were not identical. Therefore we here compared conventional tail current analyses at the same patch and found $V_{1/2}$ = –89.4 3.7 mV during and –94.4 mV ± 4.6 mV after I_h amplitude reduction (n = 6, p = 0.09 Wilcoxon signed rank test, Fig. 2B). Because during the process of I_h reduction each hyperpolarization might likewise influence gating, conventional analysis of voltage dependence of I_h activation might be inaccurate, i.e. the voltage dependence might be shifted during the recording. Therefore we reduced the number of activations to two, one at assumed medium (at –95 mV) and the other at assumed maximal (at –130 mV) activation level, and compared tail current (at –65 mV) ratios before and after I_h amplitude reduction. If voltage dependence of I_h activation was unaffected by repetitive activation, this ratio should remain similar. In our experiments, on the contrary, tail current ratios were reduced (0.49 ± 0.07 to 0.35 ± 0.06, n = 12, p < 0.001, paired t test) and had a tendency towards reduction even at assumed moderate levels of first activation (–80 mV: 0.2 ± 0.07 to 0.03 ± 0.02, n = 10, p = 0.01, Wilcoxon-signed rank test, Fig. 2C). Holding currents were equal (first steps – 95 mV: $I_{holdini}$ = 0.24 ± 0.2 pA *vs.* 0.25 ± 0.13 pA, n = 12, p = 0.98, paired t test; first steps –80 mV: $I_{holdini}$ = 0.12 ± 0.22 pA *vs.* –0.08 ± 0.21, n = 10, p = 0.08, Wilcoxon-signed rank test).
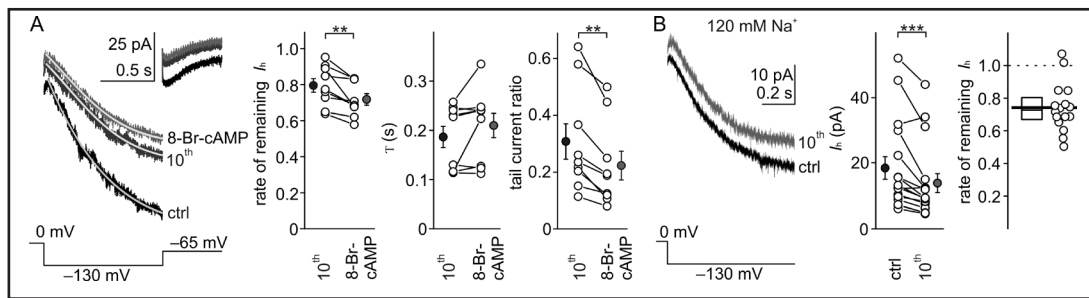
Supporting an activity induced shift in voltage dependence of rHCN1, I_h activation kinetics - another voltage dependent parameter - decelerated markedly in cell-attached mode (from τ = 268.9 ± 26.7 ms to τ = 317.1 ± 25.3 ms, n = 23, p < 0.001, paired t test, Fig. 2D), but not in whole-cell mode (τ = 180.9 ± 42.0 ms and τ = 159. ± 33.2 ms, n = 13, p = 0.17, Wilcoxon-signed rank test) after 10 consecutive activations.

Taken together, these data suggest that a hyperpolarizing shift in voltage dependence of I_h gating associates with and might support I_h amplitude reduction. However, this shift cannot explain reduction of maximum I_h amplitude and therefore not be the sole underlying cause.

Neither supramaximal intracellular cAMP nor elevated pipette sodium levels altered I_h attenuation

Use dependent attenuation of I_h mimics all features of scarce cAMP action on HCN2 and 4 channels, in particular i) hyperpolarizing shift in voltage dependence, ii) slowing of activation and iii) reduction of maximal I_h [2, 32]. Therefore we studied whether cAMP reduction underlies use dependent attenuation of rHCN1 mediated I_h, although HCN1 channels are commonly regarded as only marginally influenced by cAMP. After induction of I_h attenuation by alternating one second long voltage steps to –95 mV and –130 mV for 10 cycles in cell-attached mode we saturated intracellular cAMP levels by bath application of 100 µM of the membrane permeable and non-degradable 8Br-cAMP. This treatment did not reverse or restrict the I_h attenuation (Fig. 3A). On the opposite, 8Br-cAMP application did not prevent a slight further I_h amplitude reduction (I_{hini} = 39.3 ± 12.5 pA to I_{h10} = 33.9 ± 9.6 pA, n = 9, p < 0.01, Wilcoxon-signed rank test) also reflected in the reduction of the rate of remaining I_h (from 0.79 ± 0.03 to 0.71 ± 0.03, n = 9, p < 0.01, Wilcoxon-signed rank test). This was accompanied by a shift in voltage dependence of I_h activation as indicated by a slight further reduction in tail current ratios after 8Br-cAMP application (from 0.3 ± 0.06 to 0.2 ± 0.05, n = 9, p < 0.01, Wilcoxon-signed rank test). The activation time constant was τ = 186.3 ± 21.5 ms after use dependent I_h reduction and τ = 209.8 ± 24.6 ms after 8Br-cAMP application

KARGER

Cellular Physiology and Biochemistry

Cell Physiol Biochem 2016;38:2079-2093

DOI: 10.1159/000445566
Published online: May 17, 2016

© 2016 The Author(s). Published by S. Karger AG, Basel
www.karger.com/cpb

2087

Barthel/Reetz/Strauss: HCN1 Use Dependence

Fig. 3. Neither intracellular cAMP elevation recovered, nor high extracellular Na^+ increased I_h reduction in cell-attached mode. (A) Left: Representative traces of I_h elicited by –130 mV voltage steps after establishing the cell-attached configuration (*ctrl;* black dots), after 10 repetitive stimulations (dark grey dots) and after 3 min 100 µM 8Br-cAMP (light grey dots). Continuous lines indicate fits to single exponential functions. Right: Population data on rate of remaining I_h normalized to initial I_h amplitudes (left panel), time course of I_h activation represented as activation time constant (τ, middle panel) and tail current (–65 mV) ratios following pre-pulses of –95 mV and –130 mV (right). Depicted are values after 10 activations by 1 second –100 mV voltage steps (mean: dark grey circles) versus after 8Br-cAMP application (mean: grey circles), respectively. (B) Extracellular [Na^+] elevation did not alter I_h reduction. *Left:* Example I_h traces elicited by –130 mV voltage steps with 120 mM Na^+ in the pipette solution. Middle and right: Population data illustrate the reduction of I_h amplitudes and the rate of remaining I_h.

(n = 9, p = 0.07, Wilcoxon-signed rank). Holding currents remained comparable: $I_{holdini}$ = 0.37 ± 0.21 pA *vs.* $I_{hold8BrcAMP}$ = 0.17 ± 0.19 pA, p = 0.28, paired t test.

An apparent use dependent block of I_h without a shift in its voltage dependence was recently described during high extracellular Na^+ levels [28]. However, experimental conditions differed substantially, namely that group overexpressed HCN2 channels in *Xenopus* oocytes and conducted two electrode voltage clamp recordings. Although we observed substantial I_h attenuation with K^+ as major cation in the pipette, we repeated our cell-attached patch clamp experiments with pipette (extracellular) solution containing high [Na^+] to exclude any ion specific effects, in particular because high extracellular K^+- concentration modifies HCN channel activation kinetics and permeability [30, 33]. To that purpose we filled our pipettes with extracellular solution containing 120 mM Na^+. Activation under that condition reduced the amplitude of rHCN1 mediated I_h: alternating 1-second hyperpolarizations to –95 and –130 mV attenuated I_h (at –130 mV from 18.5 ± 3.4 pA to 13.9 ± 2.8 pA, n = 16, P = 0.01; paired t test) and the rate of remaining I_h (0.74 ± 0.04, n = 16, Fig. 3B). The holding currents remained comparable ($I_{holdini}$ = –0.004 ± 0.06 pA *vs.* I_{hold10} = 0.005 ± 0.07, n = 16, p = 0.9, paired t test).

This reduction (25.8 ± 3.7%, n = 16, p < 0.001, Wilcoxon-signed rank test) was similar to the one with K^+ as predominant cation in the pipette recorded under the same conditions, i.e. using the same pulse protocol (p = 0.38, t test). Likewise, activation time course slowed from 275.6 ± 36.0 ms to 331.2 ± 37.9 ms, p < 0.001, n =16, paired t test), again comparable to the situation with K^+ as predominant cation on the extracellular face of the patch (25.2 ± 6.6% *vs.* 29.1 ± 10.3%, respectively, p = 0.8, Mann Whitney U test).

In summary, neither alterations in intracellular cAMP nor the kind of channel permeant cations account for the use dependent I_h attenuation.

Ceasing I_h attenuation and enabling aspects of voltage dependent hysteresis under whole-cell recording conditions

Use dependence of I_h attenuation indicates conformational changes that might request reopening of the channel to be released. Therefore we reassessed our finding that I_h increase after establishing the whole-cell mode depends on solution exchange but not on channel activation [12]. We now set the holding potential to +40 mV to exclude any channel activation and applied moderate activating pulses to prevent possible effects of strong hyperpolarization, such as voltage hysteresis. Under this conditions neither I_h (I_{hini} = 905.9

KARGER
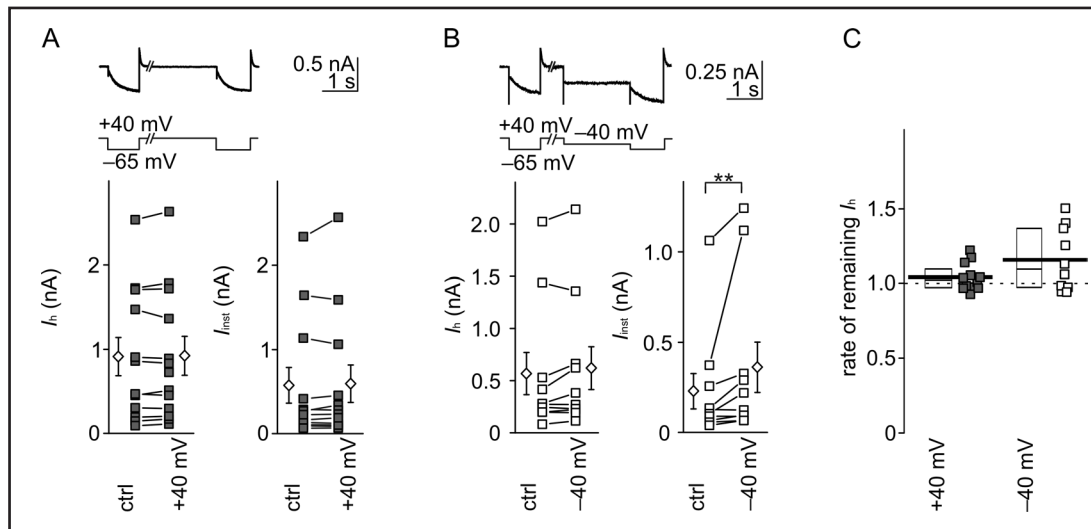
Fig. 4. Release from inactivation by exchange of cytosolic content is time dependent and voltage hysteresis is partially established. (A/B) Upper row: Example traces of whole-cell voltage clamp recordings of rHCN1 mediated I_h. Recordings started 2 - 3 minutes subsequent to rupturing the membrane. We set the holding potential to +40 mV and activated I_h by –65 mV for 1 second. Following a break of 3 minutes at +40 mV (A) or such a break ending with a non-activating pre-pulse to –40 mV for 2 seconds (B), I_h was again activated for 1 second by clamping the membrane to –65 mV. Lower row: Population data on I_h and I_{inst} elicited from a membrane voltage of +40 mV (*ctrl*) and subsequently from +40 mV (grey square line series, left panels) or –40 mV (white square line series, right panels; all means as white rhombi). (C) Comparison of rates of remaining I_h following +40 mV (grey circles) or –40 mV (white circles).

± 227.3 pA to $I_{hsecond}$ = 915 ± 231.2 pA, n = 12, p = 0.56, paired t test) nor I_{inst} amplitude ($I_{instini}$ = 572 ± 212.7 pA to $I_{instsecond}$ = 591.7 ± 223.5 pA, n = 12, p = 0.8, Wilcoxon signed rank test) differed, comparing the first hyperpolarization 3 minutes after establishing whole-cell mode (when the fast increase of I_h due to equilibration of cytosol and pipette contend had ceased [12], with a second, another 3 minutes later (Fig. 4A). In line, the time course of I_h activation at both hyperpolarizations was similar ($\tau_{actfirst}$ = 347.3 ± 57 ms *vs.* $\tau_{actsecond}$ = 329.6 ± 45.4 ms; n = 12, p = 0.68, paired t test). The holding currents remained comparable ($I_{holdini}$ = 1.13 ± 0.95 pA. *vs.* $I_{holdsecond}$ = 1.2 ± 1.0 pA, n = 12, p = 0.43, Wilcoxon signed rank test).

Interestingly, a 2 second pre-pulse to –40 mV (not activating rHCN1 mediated I_h [12]) prior to the second hyperpolarization tended to increase I_h amplitude (I_{hini} = 568.2 ± 202.3 pA to $I_{hsecond}$ = 619.4 ± 205.1 pA, n = 10, p = 0.13, Wilcoxon signed rank test) and increased I_{inst} ($I_{instini}$ = 230.8 ± 98 pA to $I_{instsecond}$ = 363.6 ± 139.6 pA, n = 10, p < 0.01, Wilcoxon signed rank test, Fig. 4B). It also markedly accelerated the activation time course of I_h (from $\tau_{act-40mV}$ = 386.9 ± 52.6 ms to $\tau_{act-40mV}$ = 282 ± 31.1 ms, n = 10, p < 0.05, paired t test). This is consistent with a voltage dependent hysteresis as described for certain HCN channels [11]. The holding currents remained comparable ($I_{holdini}$ = 52.9 ± 12.4 pA. *vs.* $I_{holdsecond}$ = 66.0 ± 13.9 pA, n = 10, p = 0.06, paired t test).

Taken together, disrupting the intracellular content under whole-cell conditions ceased activity dependence and partially enabled voltage dependent hysteresis. This is also reflected in the respective rates of remaining I_h (1.04 ± 0.03, n = 12 and 1.15 ± 0.07, n = 10, without and with a non-activating pre-pulse, respectively, Fig. 4C).

Discussion

Against the background of conflicting findings on the impact of pre-activation on HCN1 mediated I_h we here investigated biophysical consequences of repetitively activating I_h

KARGER

Cellular Physiology and Biochemistry

Cell Physiol Biochem 2016;38:2079-2093

DOI: 10.1159/000445566
Published online: May 17, 2016

© 2016 The Author(s). Published by S. Karger AG, Basel
www.karger.com/cpb

2089

Barthel/Reetz/Strauss: HCN1 Use Dependence

in mammalian cells heterologously expressing rHCN1. Our data indicate that i) recurring activation use-dependently attenuates rHCN1 mediated I_h in intact HEK293 cells (cell-attached mode) but not when the cytosol is permanently disrupted (whole-cell mode), ii) voltage of pre-activations is less important for the amount of attenuation if rHCN1 channels were activated at all, iii) I_h attenuation might be linked to voltage sensor alterations because slowly activating components of rHCN1 mediated currents were more affected than instantaneous components and gating shifts to more negative voltages after pre-activation, iv) cAMP does not affect I_h attenuation, v) the amount of I_h attenuation is irrespective of the permeating cation and vi) disrupting the cytosol partially reversed I_h attenuation to voltage hysteresis, that is facilitation of subsequent I_h following activating pre-pulses due to conformational changes in the pore stabilizing S4 in its current position [34].

The apparent use-dependence links I_h attenuation to the gating process and suggests that changes occur while ions flow through open channels. Therewith our data are consistent with the assumption that the HCN pore is involved in gating [30, 31]. Although the alterations are reminiscent of outer pore changes [31], we regard an involvement of the outer pore unlikely for two reasons: first, to rule out possible mutations during the expansion in E. coli we re-sequenced the rHCN1 construct, ending up with a proper amino acid sequence and second, the I_h attenuation did not persist in whole-cell mode, pointing to a necessity of intracellular factors. Nevertheless, we cannot fully exclude alterations in tertiary structure or in membrane insertion. Interestingly, our findings phenotypically resemble the pre-pulse dependent inactivation of sperm HCN (spHCN) channels of the sea urchin and HCN2 mediated I_h in HEK293 cells [35]: Although our pre-pulses were not directly followed by test-pulses and the pre-pulses were much shorter, subsequent pulses activated slower, maximum I_h was slightly reduced and cAMP had nearly no effect on both facets of I_h attenuation. This suggests the involvement of the assumed coupling mechanism between voltage sensor and gate [31] in rHCN1 channels, too.

Persistence and even slight augmentation of use-dependent I_h attenuation in the presence of saturating cAMP is compatible with the low cAMP sensitivity of HCN1 [36] and with the idea that cAMP does not eliminate the inactivated state, but favors the equilibrium from closed activated into an open state [35]. In contrast to HCN2 [35], rHCN1 channels did not only not recover, instead I_h attenuation accumulated. Therefore, if an uncoupling or slippage between voltage sensor and gate underlies pre-activation induced changes in HCN1 mediated I_h, it might not be temporary. Despite this slight incongruity to the gate slippage (closed state stabilization) hypothesis [35], we propose that I_h attenuation for rHCN1 channels might be due to favoring a (re)-closure of the intracellular activation gate, similar to HCN2 and spHCN channels, that is, it desensitizes to voltage. Reduction of channel number by endocytosis or "forced" lateral diffusion of channels out of the patched membrane might contribute to the amplitude attenuation.

The obvious difference in I_h attenuation between the recording modes suggests an involvement of intracellular components that are either lost or compromised by exchanging cytosol and pipette solution. During the last years the number of known cytoplasmatic components regulating I_h properties steadily increased and include intracellular metabolites [37, 38], covalent post-translational channel modulators [39-41] and auxiliary subunits [42]. Of all these neuronal precursor cell expressed developmentally downregulated (Nedd)4-2 may be a likely candidate because it is endogenously and substantially expressed in HEK293 cells, it reduces surface expression of HCN1 in HEK293 cells and I_h amplitude in *Xenopus laevis* oocytes and it shifts I_h activation to more negative voltages [43]. Mechanistically, rHCN1 activation might lead to conformational changes that ease (trigger) Nedd4-2 - rHCN1 interaction resulting in increased ubiquitination and reduced glycosylation of the channel protein. Whereas ubiquitination might contribute to the dynamic regulation of the number of rHCN1 channels in the membrane [44], glycosylation changes may influence voltage sensitivity and gating of channels by influencing electrically charged sugar moieties and therewith the extracellular electrical field. The latter has so far only been shown for certain sodium channels [45]. We suppose that posttranslational modifications would be fast enough,

KARGER

Cellular Physiology and Biochemistry

Cell Physiol Biochem 2016;38:2079-2093

DOI: 10.1159/000445566
Published online: May 17, 2016

© 2016 The Author(s). Published by S. Karger AG, Basel
www.karger.com/cpb

2090

Barthel/Reetz/Strauss: HCN1 Use Dependence

since available data suggest that for instance ubiqiutination can occur within milliseconds [46]. However, given the fast time course it might also just be removal (disruption) of post-translational modification, e. g. de-ubiquitination, de-phosphorylation or de-glycosylation. The mechanistic proposals rely merely on coincidence because the data we present do not justify claiming a causal relationship.

Alternatively, hyperpolarizations might cause a stronger interaction of HCN1 with filaminA resulting in hyperpolarized voltage sensitivity and slower activation kinetics of I_h [47]. Moreover, filaminA reversibly and selectively internalizes HCN1 channels, accumulates them in the endosome [48] and is natively present in HEK293 cells [49]. The major auxiliary tetratricopeptide repeat-containing Rab8b interacting protein (TRIP8b) is unlikely to contribute to use dependent I_h attenuation, although it is influenced by (neuronal) activity and it shifts the voltage dependent activation of HCN channels to more negative potentials as well as slows channel opening [4, 42] because TRIP8b is not natively present in HEK293 cells and would increase I_h amplitudes. Putative HCN1 interactions with these or other proteins might further complicate the situation in neurons and *in vivo*.

Other possible scenarios appear less plausible to us: I_h decline under whole-cell recording conditions, also known as run down [3], had been attributed to experimental conditions as dilution of cytoplasmic ATP, cAMP, PIP_2 [38] or improper control of intracellular Ca^{2+}, that do not apply for our cell-attached approach. Therefore, run down is very unlikely but not entirely impossible given that attempts to recover rHCN1 channels from use-dependent reduction failed. It also seems unlikely that reduction of I_h is directly due to lack of energy supply and subsequently channel activators such as cAMP, because membrane patches and therewith numbers of activated channels were rather small (404.5 ± 56.8 channels per patch, given single channel currents of about 88 fA [50]. However, I_h attenuation did not occur in *Xenopus* oocytes that have high intracellular cAMP levels [34]. Another possible link between channel activation and I_h attenuation might imply Ca^{2+} influx through open rHCN1 channels [51]. Although the fraction of Ca^{2+} in the total current is very low (for HCN4, expressed in HEK293 cells: 0.6 ± 0.002 % [51]) and the time of channel activation should determine the amount of effect (which was not the case in our experiments), Ca^{2+} influx might still activate surrounding proteolytic enzymes (as for acetylcholine receptor loss [51]) or protein kinase C (PKC) endogenously expressed in HEK293 cells [52]. Although activation of PKC reduces HCN1 mediated I_h [18], under certain experimental conditions even accompanied by a shift of I_h voltage dependence to more negative potentials [4], it cannot account for I_h attenuation in our case because the voltage sensitivity of rHCN1 in HEK293 was unperturbed by PKC increase [18]. Finally, as inherent to all cell-attached recordings [53], the depolarizing voltage response generated by HCN activation might decrease the transmembrane voltage and thereby the hyperpolarization sensed by HCN1 channels [54]. However, although probably contributing to the effect described here, we consider this unlikely to be responsible for the entire effect, because a) the amount of reduction is not voltage dependent and long activations have not the same effect as repetitive ones, b) the effect persists long beyond the cessation of HCN currents and c) reduced currents were slowed, not accelerated as in [54].

Because HCN channels are important regulators of neuronal excitability even slight changes in their properties impair proper neuronal function and may contribute to certain neurological diseases [13-16]. As depolarization by NMDA or AMPA receptors increases I_h amplitude due to increased membrane insertion [55] we speculate that hyperpolarization induced I_h attenuation might provide a counterbalance. Because of unknown content of dendritic compartments and putative heteromerization of HCN subunits, direct studies in neurons are challenging and may be hard to interpret. HEK293 may serve as useful expression system for controlled investigation of these basic principles. These findings might be relevant not only for neurons but also for cardiomyocytes. The latter could be tested particularly in induced pluripotent stem cell derived cardiomyocytes, where HCN1 is present in high levels [56].

KARGER

Cellular Physiology and Biochemistry

Cell Physiol Biochem 2016;38:2079-2093

DOI: 10.1159/000445566
Published online: May 17, 2016

© 2016 The Author(s). Published by S. Karger AG, Basel
www.karger.com/cpb

2091

Barthel/Reetz/Strauss: HCN1 Use Dependence

Acknowledgements

Disclosure Statement

The authors declare no conflict of interest.

References

1   Decher N, Chen J, Sanguinetti MC: Voltage-dependent gating of hyperpolarization-activated, cyclic nucleotide-gated pacemaker channels: molecular coupling between the S4-S5 and C-linkers. J Biol Chem 2004;279:13859–13865.

2   Baruscotti M, Bucchi A, Difrancesco D: Physiology and pharmacology of the cardiac pacemaker ("funny") current. Pharmacol Ther 2005;107:59–79.

3   Wahl-Schott C, Biel M: HCN channels: structure, cellular regulation and physiological function. Cell Mol Life Sci 2009;66:470–494.

4   He C, Chen F, Li B, Hu Z: Neurophysiology of HCN channels: from cellular functions to multiple regulations. Prog Neurobiol 2014;112:1–23.

5   Moosmang S, Biel M, Hofmann F, Ludwig A: Differential distribution of four hyperpolarization activated cation channels in mouse brain. Biol Chem 2015;380:975–980.

6   Tsay D, Dudman JT, Siegelbaum SA: HCN1 channels constrain synaptically evoked Ca2+ spikes in distal dendrites of CA1 pyramidal neurons. Neuron 2007;56:1076–1089.

7   Magee JC: Dendritic hyperpolarization-activated currents modify the integrative properties of hippocampal CA1 pyramidal neurons. J Neurosci 1998;18:7613–7624.

8   Wang J, Chen S, Siegelbaum SA: Regulation of hyperpolarization-activated HCN channel gating and cAMP modulation due to interactions of COOH terminus and core transmembrane regions. J Gen Physiol 2001;118:237–250.

9   Santoro B, Liu DT, Yao H, Bartsch D, Kandel ER, Siegelbaum SA, Tibbs GR: Identification of a gene encoding a hyperpolarization-activated pacemaker channel of brain. Cell 1998;93:717–729.

10 Zhou L, Siegelbaum SA: Gating of HCN channels by cyclic nucleotides: residue contacts that underlie ligand binding, selectivity, and efficacy. Structure 2007;15:655–670.

11 Männikkö R, Pandey S, Larsson HP, Elinder F: Hysteresis in the voltage dependence of HCN channels: conversion between two modes affects pacemaker properties. J Gen Physiol 2005;125:305–326.

12 Battefeld A, Bierwirth C, Li YC, Barthel L, Velmans T, Strauss U: Ih "run-up" in rat neocortical neurons and transiently rat or human HCN1-expressing HEK293 cells. J Neurosci Res 2010;88:3067–3078.

13 Herrmann S, Stieber J, Ludwig A: Pathophysiology of HCN channels. Pflugers Arch 2007;454:517–522.

14 Huang Z, Walker MC, Shah MM: Loss of dendritic HCN1 subunits enhances cortical excitability and epileptogenesis. J Neurosci 2009;29:10979–10988.

15 Nolan MF, Malleret Gl, Lee KH, Gibbs E, Dudman JT, Santoro B, Yin D, Thompson RF, Siegelbaum SA, Kandel ER, Morozov A: The hyperpolarization-activated HCN1 channel is important for motor learning and neuronal integration by cerebellar Purkinje cells. Cell 2003;115:551–564.

16 Nava C, Dalle C, Rastetter A, Striano P, de Kovel CGF, Nabbout R, Cancès C, Ville D, Brilstra EH, Gobbi G, Raffo E, Bouteiller D, Marie Y, Trouillard O, Robbiano A, Keren B, Agher D, Roze E, Lesage S, Nicolas A, Brice A, Baulac M, Vogt C, El Hajj N, Schneider E, Suls A, Weckhuysen S, Gormley P, Lehesjoki AE, De Jonghe P, Helbig I, Baulac S, Zara F, Koeleman BP, EuroEPINOMICS RES Consortium, Haaf T, LeGuern E, Depienne C: De novo mutations in HCN1 cause early infantile epileptic encephalopathy. Nat Genet 2014;46:640–645.

17 Thomas P, Smart TG: HEK293 cell line: a vehicle for the expression of recombinant proteins. J Pharmacol Toxicol Methods 2005;51:187–200.

KARGER

18 Reetz O, Strauss U: Protein kinase C activation inhibits rat and human hyperpolarization activated cyclic nucleotide gated channel (HCN)1-mediated current in mammalian cells. Cell Physiol Biochem 2013;31:532–541.

19 Ulens C, Tytgat J: Functional Heteromerization of HCN1 and HCN2 Pacemaker Channels. J Biol Chem 2001;276:6069–6072.

20 Maruoka F, Nakashima Y, Takano M, Ono K, Noma A: Cation-dependent gating of the hyperpolarization-activated cation current in the rabbit sino-atrial node cells properties of If channels, such as ionic permeation and. J Physiol 1994;477:423-435.

21 Henrikson CA, Xue T, Dong P, Sang D, Marban E, Li RA: Identification of a Surface Charged Residue in the S3-S4 Linker of the Pacemaker (HCN) Channel That Influences Activation Gating. J Biol Chem 2003;278:13647–13654.

22 Azene EM, Xue T, Marbán E, Tomaselli GF, Li RA: Non-equilibrium behavior of HCN channels: insights into the role of HCN channels in native and engineered pacemakers. Cardiovasc Res 2005;67:263–273.

23 Sakmann B, Neher E: Single-Channel Recording. Plenum Press, New York. 1983.

24 Lyashchenko AK, Tibbs GR: Ion binding in the Open HCN Pacemaker Channel Pore: Fast Mechanisms to Shape "Slow" Channels. J Gen Physiol 2008;131:227–243.

25 Ishii TM, Takano M, Xie LH, Noma A, Ohmori H: Molecular characterization of the hyperpolarization-activated cation channel in rabbit heart sinoatrial node. J Biol Chem 1999;274:12835–12839.

26 Gauss R, Seifert R, Kaupp UB: Molecular identification of a hyperpolarization-activated channel in sea urchin sperm. Nature 1998;393:583–587.

27 Proenza C, Angoli D, Agranovich E, Macri V, Accili EA: Pacemaker channels produce an instantaneous current. J Biol Chem 2002;277:5101–5109.

28 Pittoors F, Van Bogaert P: HCN2 Channels: a permanent open state and conductance changes. J Membr Biol 2015;248:67–81.

29 Xue T, Marbán E, Li RA: Dominant-negative suppression of HCN1- and HCN2-encoded pacemaker currents by an engineered HCN1 construct: insights into structure-function relationships and multimerization. Circ Res 2002;90:1267–1273.

30 Azene EM, Xue T, Li RA: Molecular basis of the effect of potassium on heterologously expressed pacemaker (HCN) channels. J Physiol 2003;547:349–356.

31 Azene EM, Sang D, Tsang S-Y, Li RA: Pore-to-gate coupling of HCN channels revealed by a pore variant that contributes to gating but not permeation. Biochem Biophys Res Commun 2005;327:1131–1142.

32 Craven KB, Zagotta WN: CNG and HCN channels: two peas, one pod. Annu Rev Physiol 200;68:375–401.

33 Macri V, Proenza C, Agranovich E, Angoli D, Accili EA: Separable gating mechanisms in a Mammalian pacemaker channel. J Biol Chem 2002;277:35939–35946.

34 Männikkö R, Elinder F, Larsson HP: Voltage-sensing mechanism is conserved among ion channels gated by opposite voltages. Nature 2002;419:837–841.

35 Shin KS, Maertens C, Proenza C, Rothberg BS, Yellen G: Inactivation in HCN channels results from reclosure of the activation gate: desensitization to voltage. Neuron 2004;41:737–744.

36 Wainger BJ, DeGennaro M, Santoro B, Siegelbaum SA, Tibbs GR: Molecular mechanism of cAMP modulation of HCN pacemaker channels. Nature 2001;411:805–810.

37 DiFrancesco D, Tortora P: Direct activation of cardiac pacemaker channels by intracellular cyclic AMP. Nature 1991;351:145–147.

38 Pian P, Bucchi A, Robinson RB, Siegelbaum SA: Regulation of gating and rundown of HCN hyperpolarization-activated channels by exogenous and endogenous PIP2. J Gen Physiol 2006;128:593–604.

39 Zong X, Eckert C, Yuan H, Wahl-Schott C, Abicht H, Fang L, Li R, Mistrik P, Gerstner A, Much B, Baumann L, Michalakis S, Zeng R, Chen Z, Biel M: A novel mechanism of modulation of hyperpolarization-activated cyclic nucleotide-gated channels by src kinase. J Biol Chem 2005;280:34224–34232.

40 Zha Q, Brewster AL, Richichi C, Bender RA, Baram TZ: Activity-dependent heteromerization of the hyperpolarization-activated, cyclic-nucleotide gated (HCN) channels: role of N-linked glycosylation. J Neurochem 2008;105:68–77.

41 Jung S, Bullis JB, Lau IH, Jones TD, Warner LN, Poolos NP: Downregulation of dendritic HCN channel gating in epilepsy is mediated by altered phosphorylation signaling. J Neurosci 2010;30:6678–6688.

KARGER

Cellular Physiology and Biochemistry

Cell Physiol Biochem 2016;38:2079-2093

DOI: 10.1159/000445566
Published online: May 17, 2016

© 2016 The Author(s). Published by S. Karger AG, Basel
www.karger.com/cpb

2093

Barthel/Reetz/Strauss: HCN1 Use Dependence

42 Santoro B, Piskorowski RA, Pian P, Hu L, Liu H, Siegelbaum SA: TRIP8b splice variants forma family of auxiliary subunits that regulate gating and trafficking of HCN channels in the brain. Neuron 2009;62:802–813.

43 Wilkars W, Wollberg J, Mohr E, Han M, Chetkovich DM, Bähring R, Bender RA: Nedd4-2 regulates surface expression and may affect N-glycosylation of hyperpolarization-activated cyclic nucleotide-gated (HCN)-1 channels. FASEB J 2014;28:2177–2190.

44 Hardel N, Harmel N, Zolles G, Fakler B, Klöcker N: Recycling endosomes supply cardiac pacemaker channels for regulated surface expression. Cardiovasc Res 2008;79:52–60.

45 Tyrrell L, Renganathan M, Dib-Hajj SD, Waxman SG: Glycosylation alters steady-state inactivation of sodium channel Nav1.9/NaN in dorsal root ganglion neurons and is developmentally regulated. J Neurosci 2001;21:9629–9637.

46 Pierce NW, Kleiger G, Shan S, Deshaies RJ: Detection of sequential polyubiquitylation on a millisecond timescale. Nature 2009;462:615–619.

47 Gravante B, Barbuti A, Milanesi R, Zappi I, Viscomi C, DiFrancesco D: Interaction of the Pacemaker Channel HCN1 with filamin A. J Biol Chem 2004;279:43847–43853.

48 Noam Y, Ehrengruber MU, Koh A, Feyen P, Manders EM, Abbott GW, Wadman WJ, Baram TZ: Filamin A promotes dynamin-dependent internalization of hyperpolarization-activated cyclic nucleotide-gated type 1 (HCN1) channels and restricts Ih in hippocampal neurons. J Biol Chem 2014;289:5889–5903.

49 Bachmann AS, Howard JP, Vogel CW: Actin-binding protein filamin A is displayed on the surface of human neuroblastoma cells. Cancer Sci 2006;97:1359–1365.

50 Kole MHP, Hallermann S, Stuart GJ: Single Ih channels in pyramidal neuron dendrites: properties, distribution, and impact on action potential output. J Neurosci 2006;26:1677–1687.

51 Yu X, Duan K-L, Shang C-F, Yu H-G, Zhou Z: Calcium influx through hyperpolarization-activated cation channels (Ih channels) contributes to activity-evoked neuronal secretion. Proc Natl Acad Sci U S A 2004;101:1051–1056.

52 Kawasaki T, Ueyama T, Lange I, Feske S, Saito N: Protein kinase C-induced phosphorylation of Orai1 regulates the intracellular Ca2+ level via the store-operated Ca2+ channel. J Biol Chem 2010;285:25720–25730.

53 Fenwick EM, Marty A, Neher E: A patch-clamp study of bovine chromaffin cells and of their sensitivity to acetylcholine. J Physiol 1982;331:577–597.

54 Williams SR, Wozny C: Errors in the measurement of voltage-activated ion channels in cell-attached patch-clamp recordings. Nat Commun 2011;2:242.

55 Noam Y, Zha Q, Phan L, Wu R-L, Chetkovich DM, Wadman WJ, Baram TZ: Trafficking and surface expression of hyperpolarization-activated cyclic nucleotide-gated channels in hippocampal neurons. J Biol Chem 2010;285:14724–14736.

56 Semmler J, Lehmann M, Pfannkuche K, Reppel M, Hescheler J, Nguemo F. Functional expression and regulation of hyperpolarization-activated cyclic nucleotide-gated channels (HCN) in mouse iPS cell-derived cardiomyocytes after UTF1-neo selection. Cell Physiol Biochem 2014;34:1199-1215.

KARGER